INFLUENCE OF SPECIMEN GEOMETRY ON DELAYED RETARDATION PHENOMENA OF FATIGUE CRACK GROWTH IN HT80 STEEL AND A5083 ALUMINUM ALLOY

K. Tanaka*, S. Matsuoka*, V. Schmidt** and M. Kuna**

*National Research Institute for Metals,
2-3-12, Nakameguro, Meguroku, Tokyo 153, Japan
**Academy of Sci. GDR, Inst. Solid State Phys.
Elect. Microscopy, 402 Halle, Weinberg, GDR

ABSTRACT

The behavior of fatigue crack growth should be independent of specimen geometry, if the value of stress intensity factor range, ΔK, is the same and the small scale yielding condition is satisfied. However, as clearly demonstrated in this study, this is not always applicable in the case of variable amplitude loading. The retardation phenomena of fatigue crack growth following a single application of an overload were investigated for HT80 steel and A5083-O aluminum alloy using the compact type (CT) specimens and the center-cracked (CC) specimens. The retardation took place more strongly in CC specimens than in CT specimens. This tendency appeared more drastically in the aluminum than in the steel. It was suggested that the elastic-plastic behaviors far from the crack tip, that is, in the vicinity of the elastic-plastic zone boundary would affect the retardation.

KEYWORDS

Fatigue crack growth; HT80 steel; A5083-O aluminum alloy; compact type specimen; center-cracked specimen; overload; delayed retardation; crack closure; stretch zone.

INTRODUCTION

One of the basic assumptions on the application of linear fracture mechanics to elastic-plastic materials is that plastic deformation at the crack tip is governed predominantly by the stress intensity factor, K. However, even when the value of K is the same and the small scale yielding condition is satisfied, the stress state at the crack tip depends on specimen geometry or the ratio between the applied tensile and bending stresses (Larsson and Carlsson, 1973; Heyer and MacCabe, 1972; Kuna and co-workers, 1978). Larsson and Carlsson (1973) determined the plane strain elastic-plastic states at a crack tip for various types of specimens using the finite element method (FEM). Figure 1 shows the configuration of plastic zones attending the crack tips com-

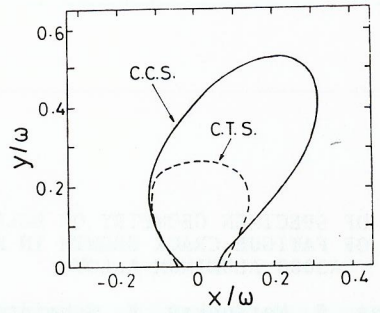

Fig.1. Plastic zones for CC and CT specimens computed by Larsson and Carlsson (1973).

puted for compact type (CT) specimen and center-cracked (CC) specimen. The crack lies along the x-axis and the tip situates at x = 0. The coordinates are normalized by the plastic zone size, ω, on the basis of the Dugdale model as given by

$$\omega = (\pi/8)(K/\sigma_{ys})^2, \qquad (1)$$

where σ_{ys} is the yield stress. The plastic zone sizes measured on the x-axis are almost same, while the plastic zone size in the direction of the y-axis for the CC specimen is almost three times as large as that for CT specimen. These different elastic-plastic behaviors at the crack tips may result in the different fatigue crack growth behaviors between the two types of specimens. However, this seems not yet conclusive. Due to Ohta, Kosuge and Sasaki (1978), the data of SM58Q steel obtained for CT and CC specimens under constant amplitude loading tests are consistent in the wide range of da/dN vs ΔK curves. Kobayashi and co-workers (1978) examined the ΔK_{th} values for quenched-tempered SNCM8 steels using the two types of specimens. They showed that the ΔK_{th} values for 300°C and 500°C tempered steels are almost same in both of the specimens, while those for 100°C tempered steel differ by a factor of two.

It has been demonstrated that the retardation phenomena of fatigue crack growth following a single application of an overload are very sensitive to material strength and mechanical factors such as specimen thickness and applied stress ratio (Matsuoka and Tanaka, 1978a, 1979, 1980). This is because the retardation phenomena are a transient behavior associating with the variation of load, which would be affected directly by the elastic-plastic states at the crack tip. This study investigated the retardation phenomena for two materials using CC and CT specimens. The results obtained were analyzed in relation to the states at the crack tips.

EXPERIMENTAL PROCEDURES

The materials used were quenched-tempered HT80 steel and A5083-O aluminum alloy. Their chemical compositions and mechanical properties are listed in Tables 1 and 2, respectively. The steel cyclic-softened, while the aluminum cyclic-hardened. The dimensions of CC and CT speci-

TABLE 1 Chemical compositions (wt%)

	C	Si	Mn	P	S	Cu	Ni	Cr	V	Mo
HT80 Steel	0.13	0.25	0.82	0.009	0.005	0.22	0.85	0.48	0.04	0.48

	Cu	Si	Fe	Mn	Mg	Zn	Cr	Ti
A5083-O Al alloy	0.03	0.15	0.22	0.72	4.71	0.01	0.12	0.01

TABLE 2 Mechanical properties

	Yield strength(MPa) Monotonic	cyclic	Ultimate tensile strength(MPa)	Elongation (%)
HT80 Steel	823	498	882	32
A5083-O Al	148	309	329	20

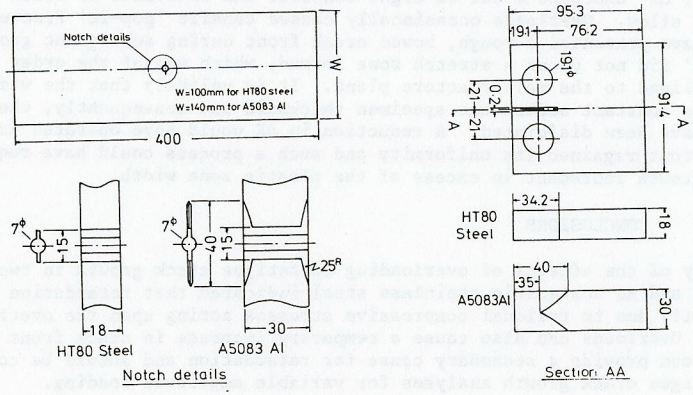

(a) CC specimen (b) CT specimen

Fig.2. Dimensions of specimens.

mens are shown in Fig.2. The retardation tests were performed under the baseline stress ratio (R) equal to zero for the CC specimens and 0.05 for the CT specimens. A single cycle of tensile overload was run manually. The applied peak stress intensity range (ΔK_2) was twice as large as the baseline stress intensity range (ΔK_1). Testing was done on 0.5MN and 0.15MN servo-hydraulic testing machines for CC and CT specimens, respectively. Cycling was interrupted periodically to measure the increment of crack extension with an optical microscope. The strainings in some CC and CT specimens were measured using two types of foil gages, which were bonded on the prolonged line of crack plane; five-element strain gages (element size: 1.4mm width x 1.0mm height, pitch: 1.8mm) positicned just in contact with the crack tips on both of the surfaces of specimens and a single element strain gage in the center of the specimen thickness at one of their sides. The former was to measure the strain distribution in the vicinity of crack tips at the application

of the overload, and the latter was to examine the crack closure behaviors by monitoring the variation in the compliance of specimens at the loading cycles during retardation (Kikukawa, Jono and Tanaka, 1976). The sizes of stretch zone produced at the overloading were examined on the fracture surfaces by a scanning electron microscope.

EXPERIMENTAL RESULTS

Figure 3 shows the fatigue crack growth curves of the two materials for the two types of specimens tested under constant amplitude loading. The calculation of ΔK value was conducted using the secant formulation (Fedderson, 1966) for CC specimens and the Newman's formulation (1974) for CT specimens. The results obtained on the different types of specimens agreed with each other within the errors of measurement in both of the materials. However, the fatigue crack growth behaviors depended on the materials. The log(da/dN) vs logΔK curves for the steel appeared linear in the range of testing, while that for the aluminum became concave upward. These data can be correlated with the equations expressed in the respective figures.

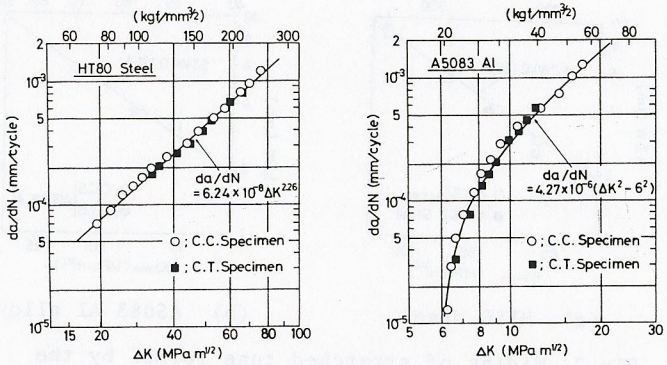

(a) HT80 steel (b) A5083 Al alloy

Fig.3. da/dN vs ΔK curves under constant amplitude loading.

The typical $(a - a_0)$ vs N curves during retardation in HT80 steel and A5083 aluminum alloy for CC and CT specimens are plotted in Fig.4, where a is the current crack length, a_0 is the crack length at the application of the overload and N is the number of cycles. The relevant ΔK_1-values as indicated in the figures were equated between both of the specimens in each material. It is evident that all samples exhibited a similar pattern of the delayed retardation (Matsuoka and Tanaka 1979b); the crack growth rate attained a minimum at the inflection points indicated by the filled marks ($a - a_0 = \omega_B$) and disappeared at the points indicated by the half-filled marks ($a - a_0 = \omega_D$). However, the retardation occurred more strongly in the CC specimens than in the CT specimens. Particularly, in the case of A5083 aluminum alloy, the number of cycles during retardation, N_D, for the CC specimen were six times as high as those for the CT specimes. It is seen in each material that the crack

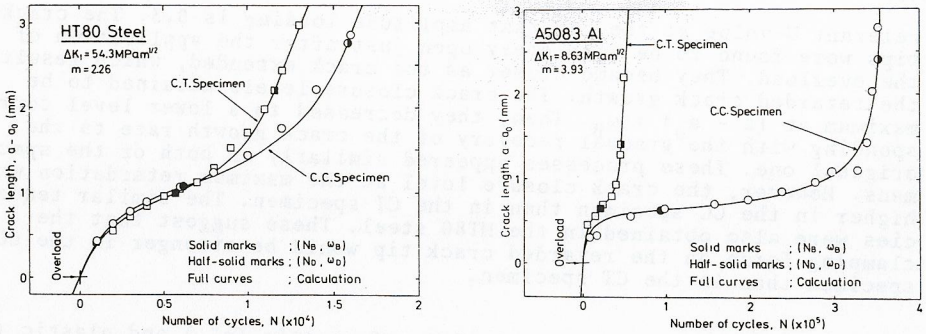

(a) HT80 steel (b) A5083 Al alloy

Fig.4. $(a - a_0)$ vs N curves during retardation.

length at the inflection point, ω_B, was almost equal, whereas the overload-affected-zone size, ω_D, was larger by about 40 per cent in the CC specimen than in the CT specimen.

Elber (1971) suggested that the retardation is caused by the increase in the crack closure level resulting from the compressive residual stresses at the crack tip induced by the overload. According to the conception, the crack growth rate, da/dN, is correlated with the effective stress intensity range, $\Delta K_{eff} = U\Delta K$, as

$$da/dN = C(\Delta K_{eff})^m = C(U\Delta K)^m, \qquad (2)$$

where U is the crack closure parameter. The experimental results in this study confirmed the Elber's suggestion as shown in Fig.5. It represents the variations in the ratio of crack opening level, $\Delta K_{op} = (1 - U)\Delta K_1$, to ΔK_1 during the retardation for the CC and CT specimens, respectively, in the A5083 aluminum alloy. In this figure, the circular marks indicate the measured values by the compliance method and the triangular marks indicate the estimated values from eqn (2) using the experimental retarded crack growth curves on the assumption that the

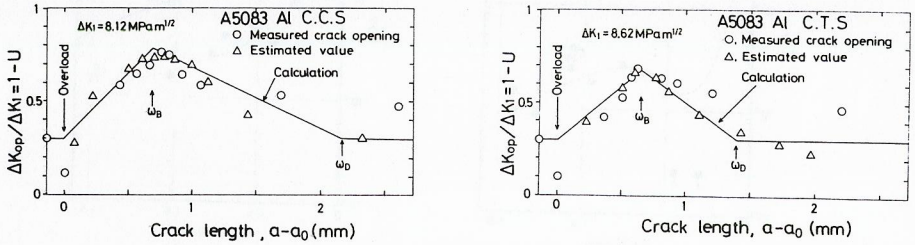

(a) CC specimen (b) CT specimen

Fig.5. Variation in crack closure level during retardation in A5083 Al alloy.

relevant U-value at the constant amplitude loading is 0.3. The crack tips were found to be completely open just after the application of the overload. They became closer as the crack extended, which resulted in the retarded crack growth. The crack closure levels attained to be maximum at $(a - a_0) \simeq \omega_B$. Then, they decreased to a lower level corresponding with the gradual recovery of the crack growth rate to the original one. These processes appeared similarly in both of the specimens. However, the crack closure level at the maximum retardation was higher in the CC specimen than in the CT specimen. The similar tendencies were also obtained in the HT80 steel. These suggest that the clamping force on the retarded crack tip would be stronger in the CC specimen than in the CT specimen.

Figure 6 represents the distributions of elastic (ε^e_{yy}) and plastic (ε^p_{yy}) strains measured at the crack tips of the CC and CT specimens in the HT80 steel on the x-axis in the coordinate of Fig.1 under the overloading of K_{2max}. The abscissa is normalized by the plastic zone size, ω_{2max}, calculated from eqn (1) using the K_{2max}-value for K and the appropriate monotonic yield strength in Table 1 for σ_{ys}. The ω_D-values obtained in the respective specimens are indicated in the relevant positions in Fig.6 by the arrow marks. It is revealed that the elastic strain in both of the specimens reduced monotonically as the increasing distance from the crack tip. However, although the reducing tendencies were almost same in the region where $x/\omega_{2max} < 0.3$ in both of the specimens, they differed significantly in the region where $x/\omega_{2max} > 0.3$; the elastic strain in the CC specimen tended to saturate in the region, while that in the CT specimen decreased rapidly as x/ω_{2max} increased. The plastic deformation occurred somewhat differently in both of the specimens. The measured plastic strains in the CT specimen decreased monotonically as the increasing distance from the crack tip, whereas those for the CC specimen became minus at $x/\omega_{2max} \simeq 0.3$ and then recovered to the same level as those for the CT specimen in the

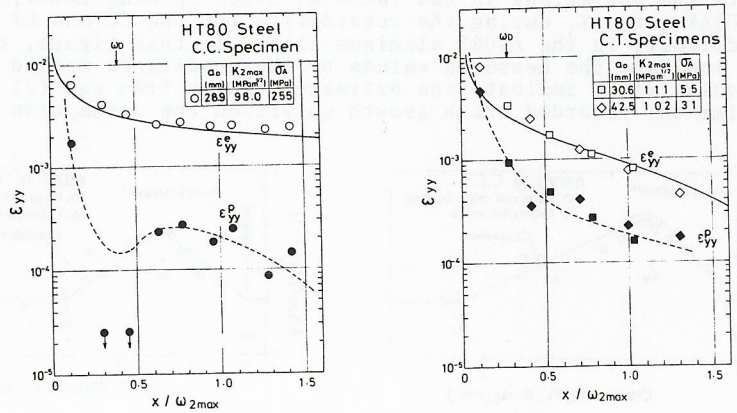

(a) CC specimen (b) CT specimen

Fig.6. Strain distributions measured at overloaded crack tips.

region where $x/\omega_{2max} > 0.5$. The latter anomalous behavior would result from the redistribution of internal stress caused by the strong plastic deformation in the region just attached to the crack tip. The plastic zone sizes would be about $0.3\omega_{2max}$ in both of the specimens, if the plastic zone is defined by the region where $\varepsilon^p_{yy} > 10^{-3}$.

Figure 7 exhibits the stretch-zone-width's (SZW's) measured on the fracture surfaces of the CC and CT specimens in HT80 steel and A5083 aluminum alloy as a function of K_{2max}. These results did not depend on the specimen geometry in both of the materials, being correlated by the following equation,

$$SZW = 0.125\delta, \text{ where } \delta = (K_{2max})^2/E\sigma_{ys}. \quad (3)$$

These facts seem to confirm the FEM analysis conducted by Larsson and Carlsson (1973) that the relevant values are 0.12δ (CT specimen) and 0.135δ (CC specimen), when the SZW is equated to half of the crack-tip-opening-displacement (Kobayashi, Nakamura and Nakazawa, 1979).

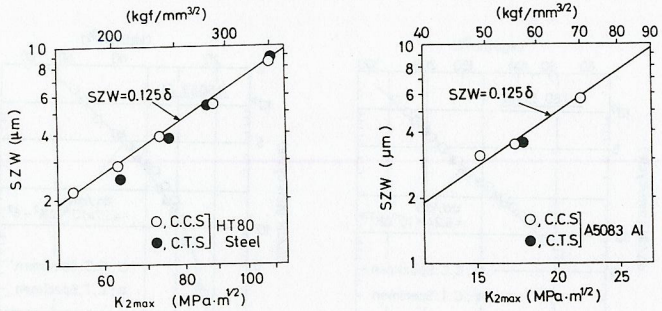

(a) HT80 steel (b) A5083 Al alloy

Fig.7. Widths of stretched zone formed by the overload.

ANALYSIS OF RETARDATION

According to Matsuoka and Tanaka's model (1979b), the number of cycles during retardation, N_D, is expressed using the exponent of the Paris equation, m, and the characteristic crack lengths, ω_B and ω_D, as

$$N_D/N_C = \{(\omega_B/\omega_D)^{1-m} - 1\}/(1 - \omega_B/\omega_D)(m - 1), \quad (4)$$

where N_C is the number of cycles required for propagation over ω_D under constant amplitude loading, i.e., $\omega_D/C\Delta K_1^m$. This model is actually based on the assumption that the crack closure behavior varies as indicated by the solid curves in Fig.5 (Matsuoka, Tanaka and Kawahara, 1976). The experimental results in Fig.4 can be correlated on this model by the solid curves, where the slopes of the log(da/dN) vs logΔK curves at the application of the overload were used as the relevant

m-values of the Paris equation. Figure 8(a) represents the N_D/N_C vs ω_B/ω_D relationships obtained for the CC and CT specimens in both of the materials. The theoretical curves calculated from eqn (4) are shown in the figure for the cases when m = 2, 3 and 4. For the HT80 steel, the m-value was constant and equal to 2.26, and thus, the experimental N_D/N_C-values obtained by the tests with different ΔK_1-values positioned nearly along the curve of m = 2. The tests for CC specimens of A5083 aluminum alloy were conducted in the range of ΔK_1-values between 7.6 and 10.9MPam$^{1/2}$ and thus the corresponding m-values varied between 2.9 and 5.5. The tests for CT specimens of the same material were done under the constant ΔK_1-value equal to 8.6MPam$^{1/2}$ varying the length of crack, a_0, between 27.8 and 39.1mm. Figure 8(b) exhibits the ω_D/ω_2 vs ω_2/B relationships, where B is the thickness of specimen and ω_2 is the plastic zone size computed from eqn (1) by using ΔK_2 for K. The value of ω_2/B may indicate a measure of the constraint to the plastic deformation at a crack tip. The ω_D/ω_2-values of the HT80 steel for both specimens showed a slight decrease as the increasing ω_2/B-value, while those of the A5083 aluminum alloy for the CT specimens did a steep increase. Moreover, the latter decreased as the increasing crack length, a_0, at the constant ΔK_1-value. It is obvious from Fig.8 that the N_D/N_C-values for the CC specimens were larger than those for the CT specimens because of the higher ω_B/ω_D-values, which mainly resulted from the higher ω_D/ω_2-values. This tendency appeared more distinctly in A5083 aluminum alloy because of the higher m-values.

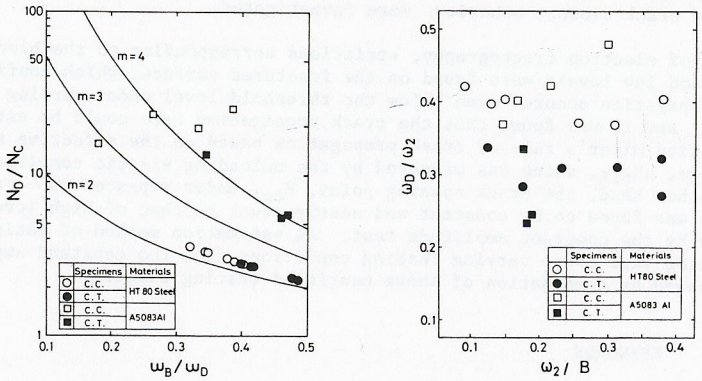

(a) N_D/N_C vs ω_B/ω_D.

(b) ω_D/ω_2 vs ω_2/B.

Fig.8. The analytical results of retardation.

DISCUSSION

In the case of a CC specimen, the elastic stresses at the crack tip on the x-axis in the coordinate system as shown in Fig.1 are given analytically by (Williams, 1957)

$$\sigma_{xx} = K/(2\pi x)^{1/2} - \sigma_A, \qquad \sigma_{yy} = K/(2\pi x)^{1/2}, \tag{5}$$

where σ_A is the applied stress and equal to P/WB (P: the applied load, W: the specimen width). Those for a CT specimens were computed by the FEM (Kuna, 1977) at a = W/2. The results can be approximated by the following formulation;

$$\sigma_{xx} = K/(2\pi x)^{1/2} - 12\sigma_A(x/a) + 1.2\sigma_A, \qquad \sigma_{yy} = K/(2\pi x)^{1/2} - 12\sigma_A(x/a) - 3.2\sigma_A. \tag{6}$$

These formulations were confirmed by the strain gage measurements on the CC and CT specimens in the HT80 steel as shown in Fig.6. The solid curves in the figure were the elastic strains, $\varepsilon^e_{yy} = (\sigma_{xx} - \nu\sigma_{yy})/E$, computed from eqns (5) and (6), respectively, using E = 206GPa and ν = 0.3. The theoretical curves agreed excellently with the experimental results.

It is evident in Fig.5 that the retardation was intimately related to the crack closure behavior. Matsuoka, Tanaka and Kawahara (1976) suggested that the overload affects the crack tip in two different ways, resulting in the different crack closure behaviors. The residual plastic strain left by the overload tends to close the crack tip. This closing force is expected to be maximum just after the application of the overload. On the other hand, the geometric blunting of the crack tip, which delays the occurrence of the maximum retardation up to the inflection point, ω_B. The results in Fig.7 show that the SZW's of CC and CT specimens were almost equal in both of the materials. Since the SZW is a measure of crack tip blunting, it may be concluded that the blunting of the crack tip was independent of the specimen geometry. As indicated in Figs.4 and 7, this resulted in that the initial delay of the retardation occurred very similarly in both of the specimens. However, it seems that the closing force was different between the CC and CT specimens. According to Larsson and Carlsson's calculation (1973) as shown in Fig.1, the plastic zone in the y-direction is much larger in CC specimen than in CT specimen. Therefore, the plastic constraint against the plane normal to the crack becomes larger, although this was not certain in the results of the strain gage measurements in Fig.6. The clamping of the residual plastic strain would be controlled by the elastic force normal to the crack plane in front of the crack tip or σ_{yy}, since the internal stress field induced by the application of the overload should be balanced by the applied stress field, σ_{yy}. As is realized by comparing eqn (5) with eqn (6), the amount of σ_{yy} for CC specimen becomes relatively larger than that for CT specimen as the increasing distance from the crack tip. This will result in the stronger crack closure or the larger overload-affected-zone size in CC specimen than in CT specimen as is shown in Figs.4 and 8. One of the evidences resides in the fact that, as is indicated in Fig.6, the overload in both of the specimens finished at a position in the vicinity of the elastic-plastic zone boundary having the equal amount of elastic strain, ε^e_{yy}.

SUMMARY

The delayed retardation phenomena of fatigue crack growth following a single application of an overload were investigated for quenched-tempered HT80 steel and A5083-O aluminum alloy using the compact type (CT) specimens and the center-cracked (CC) specimens. The fatigue

crack growth behaviors under constant amplitude loading for both specimens were in good agreement with each other in both materials. The retardation occurred more strongly in the CC specimens than in the CT specimens, when the baseline stress intensity ranges were the same. This tendency appeared more clearly in the aluminum than in the steel. This was attributed to the difference in the overload-affected-zone size, which would be affected by the elastic-plastic behaviors in the vicinity of the elastic-plastic zone boundary rather than those just attached to the crack tip.

ACKNOWLEDEGMENT

This study was done during the time when one of the authors (V. Schmidt) stayed in NRIM as a foreign specialist invited by Japanese Science and Technology Agency.

REFERENCES

Elber, W. (1971). ASTM STP486, 230 - 242.
Fedderson, R. E. (1966). ASTM STP410, 77.
Heyer, R. H., D. E. McCabe (1972). Engng Fract. Mech., 4, 413 - 430.
Kikukawa, M., M. Jono and K. Tanaka (1976), Proc. ICM2, Boston, 254 - 277.
Kobayashi, H., K. Fujita, A. Komine and H. Nakazawa (1978). Pre-print of the annual meeting of JSME (Japan), No.780-4, 113 - 115.
Kobayashi, H., H. Nakamura and H. Nakazawa (1979), Proc. ICM3, Cambridge, England, 529 - 538.
Kuna, M. (1977). Anwendung der Methode der Finiten Elemente auf Probleme der Bruchmechanik, Dissertation, Halle, GDR.
Kuna, M., Z. Bilek, Z. Knést and V. Schmidt (1978). Czech. J. Phys., B28, 88 - 108.
Larsson, S. G., and A. J. Carlsson (1973). J. Mech. Phys. Solid, 21, 263 - 277.
Matsuoka, S. and K. Tanaka (1978a). J. Mat. Sci., 13, 1335 - 1353.
(1978b). Engng Fract. Mech., 10, 515 - 525.
(1979). Engng Fract. Mech. 11, 703 - 715.
(1980). Engng Fract. Mech., on press.
Matsuoka, S., K. Tanaka and M. Kawahara (1976). Engng Fract. Mech., 8, 507 - 523.
Newman, Jr. J. C. (1974). ASTM STP560, 105 - 121.
Ohta, A., M. Kosuge and E. Sasaki (1978). Pre-print of the annual meeting of JSME (Japan), No.780-4, 9 - 11.
Williams, M. L. (1957). J. appl. Mech., 24, 109.